International Journal of Automation and Computing 13(4), August 2016, 401-408
DOI: 10.1007/s11633-016-0994-2

Operator-based Nonlinear Temperature Control Experiment for Microreactor Group Actuated by Peltier Devices

Shotaro Kawahata Ming-Cong Deng
The Graduate School of Electrical and Electronic Engineering, Tokyo University of Agriculture and Technology, Tokyo 184-8588, Japan

Abstract: In this paper, operator-based nonlinear water temperature control for a group of three connected microreactors actuated by Peltier devices is proposed. To control the water temperature of tube in the microreactor, the temperature change of aluminum effects is considered. Therefore, the temperature change of aluminum becomes the part of an input of the tube. First, nonlinear thermal models of aluminum plates and tubes that structure the microreactor are obtained. Then, an operator based nonlinear water temperature control system for the microreactor is designed. Finally, the effectiveness of the proposed models and methods is confirmed by simulation and experimental results.

Keywords: Peltier device, microreactor, nonlinear control, nonlinear process modeling, operator, continuous-time systems.

1 Introduction

In metals and semiconductors, there is a phenomenon that can interconvert between heat and electricity. This phenomenon is called thermoelectric effect[1]. The element that uses thermoelectric effects is named thermoelectric element. More specifically, the different temperature produces an electric potential (voltage) which can drive an electric current in a closed circuit.

Peltier device is one of thermoelectric element devices that can get more Peltier effect by choosing the correct materials and designing the structure. They have characteristics such as generating no noises and no vibration, using no freon gas and being able to make small and light weight apparatus, and change the electric energy directly to heat. Because of their characteristics, they are used as a cooling device for central processing unit (CPU), a small refrigerator and wine cooler in recent years. It is difficult to control the Peltier devices using the general linear system control technique, because they have nonlinear factors. The controller that can control the nonlinear part must have be designed.

When we imagine a chemical experiment, most people think of the large vessels in reactors which are used in chemical and refinery plants. The reactors used in industrial field, are well known for their large size. However, chemical engineers are finding that a new smaller type of reactor can be more useful than the traditional reactors. These reactors are called microreactors[2, 3]. A microreactor is one of the several chemical engineering unit process devices that are designed at the micrometer scale. It has some characteristics such as small size, large surface area per unit volume. The flow of liquid inside the microreactor is steamline flow. From these characteristics, it has received much attention from the fields of chemical engineering and biotechnology as a new production equipment.

There are three modes of heat transfer, which are conduction, convection and radiation. Heat conduction is a phenomenon that heat moves from high temperature to low temperature caused by movement of free electrons. To formulate the heat conduction as a mathematical expression, there is a law called "Fourier′s law". Convection is a heat movement between solid and fluid represented by air and water. To make mathematical expression, there is a law named "Newton law of cooling". Radiation is a heat transfer due to emission of electromagnetic waves, named "Stefan-Boltzmann law".

Peltier elements have complex structural limitations, such as the input voltage and the cooling capacity. Of course, modeling dynamics of Peltier element is also difficult because Peltier devices have high nonlinear properties[4]. For the nonlinear device, analysis, design and control of this kind of process are difficult. Many approaches have been proposed to control some process with nonlinear properties. In recent years, it is well known that the operator-based approach has been a promising approach for nonlinear system[5, 6]. Based on the operator theory, the stability of nonlinear system can be analyzed easily[7, 8]. Especially, it is well known that operator-based robust right coprime factorization approach has been a promising approach for analysis, design, stabilization and control of nonlinear system[9−12].

Research Article
Manuscript received February 3, 2015; accepted June 16, 2015; published online June 20, 2016
Recommended by Associate Editor Victor Becerra

In the previous studies, refrigerant such as water solution was used to dissipate the heat from microreactor. However, it was unable to control it precisely and the entire system becomes bulky and vibrating.

In this research, the main purpose is to control the water temperature of tube that structures the microreactor. Specifically, considering 3 types of heat transfer, we propose accurate modeling of a microreactor thermal process with Peltier device[13−15]. Cooling system of microreactor is shown and effectiveness of the proposed system is shown by simulation results and experimental results[16].

2 Mathematical preparation

2.1 Normed linear space

Consider a space U as time functions. U is said to be a vector space when it is closed under addition and scalar multiplication. The space U_s is said to be normed if each element x in U_s is endowed with norm $\| x \|$ which fulfills the following three properties:

1) $\| x \|$ is a real, positive number and is different from zero unless x is identically zero.

2) $\|ax\| = |a|\|x\|$.

3) $\| x_1 + x_2 \| \leq \| x_1 \| + \| x_2 \| \ (x_1, x_2 \in U_s)$.

2.2 Definition of operator

Let U_s and Y_s be two normed linear spaces over the field of complex numbers, endowed, respectively, with norms $\| \cdot \|_{U_s}$ and $\| \cdot \|_{Y_s}$. Let $Q : U_s \to Y_s$ be an operator mapping from U_s to Y_s.

If the operator $Q : D(Q) \to Y_s$ satisfies addition rule and multiplication rule

$$Q : ax_1 + bx_2 \to aQ(x_1) + bQ(x_2) \tag{1}$$

for all $x_1, x_2 \in D(Q)$ and all $a, b \in C$, then Q is said to be linear. Otherwise, it is said to be nonlinear. Since linearity is a special case of nonlinearity, "nonlinear" will always mean "not necessarily linear" unless indicated.

Let $S(X, Y)$ be the set of stable operators mapping from X to Y, then $S(X, Y)$ contains a subset defined by

$$U(X, Y) = \{M : M \in \mathcal{S}(X, Y)\} \tag{2}$$

where M is invertible with $M^{-1} \in S(Y, X)$. Elements of $U(X, Y)$ are called as unimodular operators[10].

2.3 Well-posedness

Consider the problem of stabilizing a nonlinear process $P : C(U) \mapsto C(Y)$ by a controller $K : C(Y) \mapsto C(U)$. For simplicity, a feedback control system is denoted as $\{P, K\}$.

The system $\{P, K\}$ is well-posed if the closed-loop system input-output operator from u_1, u_2 to e_1, e_2, namely

$$\left[\begin{array}{cc} I & -K \\ -P & I \end{array} \right]^{-1}. \tag{3}$$

exists.

Only the systems being well-posed shall be considered in this research.

2.4 Bounded-input bound-output (BIBO) stability

The system $\{P, K\}$, assumed well-posed, is said to be ϵ_1, ϵ_2 bounded-input stable if and only if for all inputs $|u_1| < \epsilon_1$ and $|u_2| < \epsilon_2$, the outputs y_1, y_2, e_1 and e_2 are bounded. Note that internal stability is a stronger condition than bounded-input bounded-output stability.

2.5 Internal stability

The system $\{P, K\}$, which is assumed as well-posed, is said to be internally stable if, and only if, for all bounded-inputs u_1, u_2 the outputs y_1, y_2, e_1 and e_2 are bounded, i.e.,

$$\left[\begin{array}{cc} I & -K \\ -P & I \end{array} \right]^{-1} \tag{4}$$

is BIBO stable.

2.6 Lipschitz norm

Let $N(U_s, Y_s)$ be the family of all nonlinear operators mapping from $D(Q) \subset U_s$ into Y_s. Recall that $L(U_s, Y_s)$ is used to denote the family of bounded linear operators from U_s to Y_s. Obviously, $L(U_s, Y_s) \in L(U_s, Y_s)$. In the case that $U_s = Y_s$, we use the notation $L(U_s)$ and $N(U_s)$, respectively, instead of $L(U_s, U_s)$ and $N(U_s, U_s)$ for simplicity.

For D_s be a subset of U_s and $F(D_s, Y_s)$ be the family of nonlinear operators Q in $N(U_s, Y_s)$ with $D(Q) = D_s$, a (semi-)norm for (a subset of) $F(D_s, Y_s)$ is denoted by

$$\| Q \| = \sup_{\substack{x_1, x_2 \in D_s \\ x_1 \neq x_2}} \frac{\| Q(x_1) - Q(x_2) \|_{Y_s}}{\| x_1 - x_2 \|_{U_s}} \tag{5}$$

if it is finite. In general, it is a semi-norm in the sense that $\| Q \| = 0$ does not necessarily imply $Q = 0$. In fact, it can be easily seen that $\| Q \| = 0$ if and only if Q is a constant-operator (need not be zero) that maps all elements from D_s to the same element in Y_s.

Let $Lip(D_s, Y_s)$ be the subset of $F(D_s, Y_s)$ with each element Q satisfying $\| Q \| < \infty$. Each $Q \in Lip(D_s, Y_s)$ is called a Lipschitz operator mapping from D_s to Y_s, and the number $\| Q \|$ is called the Lipschitz semi-norm of the operator Q on D_s.

In this note, we assume the operators are of Lipschitz type and use semi-norm of Lipschitz operators. It is clear that an element Q of $F(D_s, Y_s)$ is in $Lip(D_s, Y_s)$ if and only if there is a number $L \leq 0$ such that

$$\| Q(x_1) - Q(x_2) \|_{Y_s} \leq \ L \| x_1 - x_2 \|_{D_s} \tag{6}$$

for all $x_1, x_2 \in D_s$.

The norm $\| Q \|$ is the least such constant L. It is also evident that a Lipschitz operator is both bounded and continuous on its domain. Basic theories of nonlinear Lipschitz operators are given in [9].

The given plant operator $P : U \to Y$ is said to have a right factorization if there exist a linear space W and two stable operators $D : W \to Y$ and $N : W \to Y$ such that D is invertible from U to W and $P = ND^{-1}$ on U. Such a factorization of P is denoted as (N, D), and the space W is called a quasi-state space of P.

Let N and D be a right factorization for $P : X \to Y$

$$P = ND^{-1}, \qquad \begin{matrix} N : W \to Y \\ D : W \to U \end{matrix} \tag{7}$$

where N and D are stable operators from the quasi-state space W to the input and output spaces. Then, (N, D) is a right coprime factorization of P if and only if for all unbounded inputs $w \in W$, $N(w)$ or $D(w)$ is unbounded.

Let (N, D) be a right factorization of $P : U \to Y$. P is said to be a right coprime factorization if there are two stable operators $S : Y \to U$, $R : U \to U$ and R is invertible, S, N, R, D satisfy the Bezout identity

$$SN + RD = L \tag{8}$$

where some $L \in \mathcal{U}(W, U)$. If $W = U$, then usually L is replaced by identity operator I.

When mapping Σ itself of a system is stable, the state space expression corresponding to an obvious left-right coprime solution is obtained. Suppose that the stable mapping Σ has state space expression like the following equation. However, suppose that the mapping $u \to (x, y)$ is stable.

$$\Sigma : \begin{cases} \dot{x} = f(x, u) \\ y = h(x, u). \end{cases} \tag{9}$$

An obvious right coprime factorization for this object is shown as

$$D : u = v \qquad N : \begin{cases} \dot{x} = f(x, v) \\ y = h(x, v). \end{cases} \tag{10}$$

2.7 Problem statement

In this section, structure of microreactor system in our laboratory is reviewed. The system is shown in Fig. 1.

The main purpose is to control the water temperature of tube in microreactor. Temperature of tube is affected from the temperature of cooled aluminum actuated by Peltier devices.

2.8 Modeling of the Peltier device

Peltier devices are the thermoelements and have a specific phenomenon called Peltier effect, one side of them has endothermic and another side has exothermic when an electric current is applied, and the hot side and cold side reverses when opposite direction of current is applied.

Modeling of the endothermic in Peltier device is discussed. u_d is an endothermic amount of Peltier device. u_d is shown as

$$u_d = ST_c i - K(T_h - T_c) - \frac{1}{2}Ri^2 \tag{11}$$

Fig. 1 Microreactor group

where $ST_c i$ is a heat caused by Peltier effect that moves from endothermic sides to exothermic sides, $K(T_h - T_c)$ is a heat movement caused by temperature gradient, $\frac{1}{2}Ri^2$ is a Joule heat in Peltier device. Considering only endothermic sides, Joule heat is half. Using (11), we consider an endothermic as positive, heat caused by Peltier effect is positive, heat movement caused by temperature gradient and Joule heat in Peltier device is negative.

Exothermic amount of Peltier device Q_h is shown as

$$Q_h = ST_h i - K(T_h - T_c) + \frac{1}{2}Ri^2. \tag{12}$$

There is an energy conservation law between endothermic and exothermic.

$$Q_h = u_d + iV. \tag{13}$$

V is shown as

$$V = Ri + S(T_h - T_c). \tag{14}$$

$S(T_h - T_c)$ means electromotive force by the Seebeck effect.

As there is a limit of power source, we need to set a limit to u_d (W). The maximum amount of endothermic and minimum amount of endothermic must be settled. The minimum amount of endothermic, $u_{d_{\min}}$ (W) is set as 0 (W). The maximum amount of endothermic is set as next equation. We use 12 (V) constant voltage power in this system, and maximum current $i_{\max}$ is

$$i_{\max} = \frac{V_{const} - S(T_h - T_c)}{R}. \tag{15}$$

Now, $V_{const} = 12$ (V). From (15), the maximum current $i_{\max}$ is designed. Then, the maximum amount of endothermic $u_{d_{\max}}$ (W) is decided by (11).

2.9 Modeling of the aluminum box

In this paper, four Peltier devices are installed on front and back sides of aluminum box. Cooling is provided for the aluminum box when an electric current is applied to the devices. The configuration of microreactor group is shown in Fig. 2 and their model is shown in Figs. 3 (aluminum part) and 4 (tube part). Their parameters are measured and shown in Table 1. S_4 indicates the surface area of the device and S_1 means the surface area of aluminum box including the devices.

Aluminum box unit is separated into 2 parts. Tube inside the microreactor is also separated into 2 parts.

Thermal conduction equation of aluminum box is shown as Part $A_n (n = 1, 2, 3, 4, 5, 6)$.

$$\text{Part } A_1: \frac{\mathrm{d}(T_0 - T_{a_1}) m_a c_a}{\mathrm{d}t} = 2u_{d_1} - \alpha(T_0 - T_{a_1})(S_1 + S_2 + S_3 - 2S_4 - S_5) - \alpha_w S_6 (T_{a_1} - T_{w_1}) + \frac{\lambda_a S_3 (T_{a_1} - T_{a_2})}{\mathrm{d}x} + \epsilon_a \sigma (T_{a_1}^4 - T_0^4)(S_1 + S_2 + S_3 - 2S_4 - S_5) \quad (16)$$

$$\text{Part } A_2: \frac{\mathrm{d}(T_0 - T_{a_2}) m_a c_a}{\mathrm{d}t} = 2u_{d_1} - \alpha(T_0 - T_{a_2})(S_1 + S_2 + S_3 - 2S_4 - S_5) - \alpha_w S_6 (T_{a_2} - T_{w_2}) + \frac{\lambda_a S_3 (T_{a_2} - T_{a_1})}{\mathrm{d}x} + \epsilon_a \sigma (T_{a_2}^4 - T_0^4)(S_1 + S_2 + S_3 - 2S_4 - S_5) \quad (17)$$

$$\text{Part } A_3: \frac{\mathrm{d}(T_0 - T_{a_3}) m_a c_a}{\mathrm{d}t} = 2u_{d_2} - \alpha(T_0 - T_{a_3})(S_1 + S_2 + S_3 - 2S_4 - S_5) - \alpha_w S_6 (T_{a_3} - T_{w_3}) + \frac{\lambda_a S_3 (T_{a_3} - T_{a_4})}{\mathrm{d}x} + \epsilon_a \sigma (T_{a_3}^4 - T_0^4)(S_1 + S_2 + S_3 - 2S_4 - S_5) \quad (18)$$

$$\text{Part } A_4: \frac{\mathrm{d}(T_0 - T_{a_4}) m_a c_a}{\mathrm{d}t} = 2u_{d_2} - \alpha(T_0 - T_{a_4})(S_1 + S_2 + S_3 - 2S_4 - S_5) - \alpha_w S_6 (T_{a_4} - T_{w_4}) + \frac{\lambda_a S_3 (T_{a_4} - T_{a_3})}{\mathrm{d}x} + \epsilon_a \sigma (T_{a_4}^4 - T_0^4)(S_1 + S_2 + S_3 - 2S_4 - S_5) \quad (19)$$

$$\text{Part } A_5: \frac{\mathrm{d}(T_0 - T_{a_5}) m_a c_a}{\mathrm{d}t} = 2u_{d_3} - \alpha(T_0 - T_{a_5})(S_1 + S_2 + S_3 - 2S_4 - S_5) - \alpha_w S_6 (T_{a_5} - T_{w_5}) + \frac{\lambda_a S_3 (T_{a_5} - T_{a_6})}{\mathrm{d}x} + \epsilon_a \sigma (T_{a_5}^4 - T_0^4)(S_1 + S_2 + S_3 - 2S_4 - S_5) \quad (20)$$

$$\text{Part } A_6: \frac{\mathrm{d}(T_0 - T_{a_6}) m_a c_a}{\mathrm{d}t} = 2u_{d_3} - \alpha(T_0 - T_{a_6})(S_1 + S_2 + S_3 - 2S_4 - S_5) - \alpha_w S_6 (T_{a_6} - T_{w_6}) + \frac{\lambda_a S_3 (T_{a_6} - T_{a_5})}{\mathrm{d}x} + \epsilon_a \sigma (T_{a_6}^4 - T_0^4)(S_1 + S_2 + S_3 - 2S_4 - S_5). \quad (21)$$

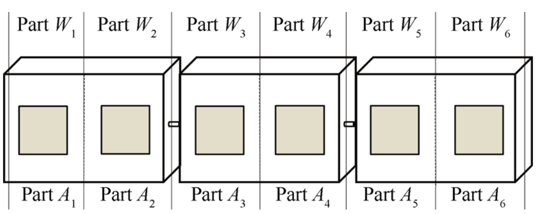

Fig. 2 Model of microreactor group

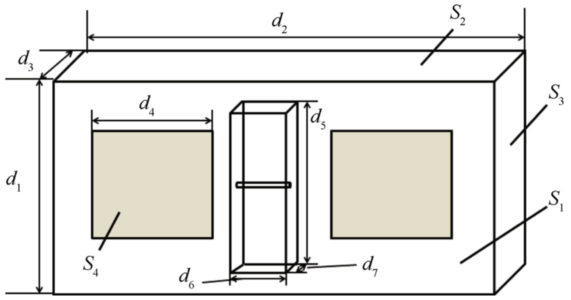

Fig. 3 Model of aluminum box

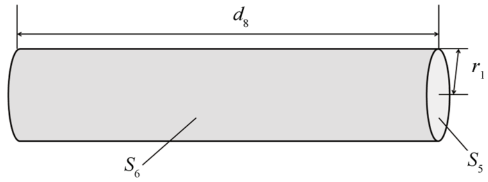

Fig. 4 Model of tube

Table 1 Parameters of microreactor

Description	Parameters
Initial temperature	T_0 (K)
Initial water temperature	T_{w_0}(K)
Temperature of endothermic side	T_c (K)
Temperature of exothermic side	T_h (K)
Temperature of Part A_n	T_{a_n}(K)
Temperature of Part W_k	T_{w_k} (K)
Current	i (A)
Peltier's Seebeck coefficient	S (V/K)
Peltier's heat conductance	K (W/K)
Peltier's resistance	R (Ω)
Emissivity of aluminum	ϵ_a (-)
Emissivity of water	ϵ_w (-)
Stefan-Boltzmann constant	σ (W/m^{2}K^4)
Heat transfer rate of air	α (W/m^{2}K)
Heat transfer rate of water	α_w (W/m^{2}K)
Thermal conductivity rate of aluminum	λ_a (W/mK)
Thermal conductivity rate of water	λ_w (W/mK)
Specific heat of aluminum	c_a (J/kgK)
Specific heat of water 4180	c_w (J/kgK)
Mass of aluminum	m_a (kg)
Mass of water	m_w (kg)

The main parameters are modeled and shown in Table 1. Define $y_{a_n} = T_0 - T_{a_n} (n = 1, 2, 3, 4, 5, 6)$, and (5) – (10) are transformed as

$$\text{Part } A_{a_n}: \frac{dy_{a_n}}{dt} = \omega_{a_n} + \sum_{m=1}^{4} (-1)^m A_{a_{nm}} y_{a_n}^m. \quad (22)$$

Here, $\omega_{a_n} (n{=}1\text{–}6)$ and $A_{a_{nm}} (n{=}1\text{–}6; m{=}1\text{–}4)$ are shown as

$$\omega_{a_1} = \frac{(2u_{d_1} + \alpha_w S_6 y_{w_1} + \frac{\lambda_a S_3 y_{a_2}}{\mathrm{d}x})}{m_a c_a} \quad (23)$$

$$\omega_{a_2} = \frac{(2u_{d_1} + \alpha_w S_6 y_{w_2} + \frac{\lambda_a S_3 y_{a_1}}{\mathrm{d}x})}{m_a c_a} \quad (24)$$

$$\omega_{a_3} = \frac{(2u_{d_2} + \alpha_w S_6 y_{w_3} + \frac{\lambda_a S_3 y_{a_4}}{\mathrm{d}x})}{m_a c_a} \quad (25)$$

$$\omega_{a_4} = \frac{(2u_{d_2} + \alpha_w S_6 y_{w_4} + \frac{\lambda_a S_3 y_{a_3}}{\mathrm{d}x})}{m_a c_a} \tag{26}$$

$$\omega_{a_5} = \frac{(2u_{d_3} + \alpha_w S_6 y_{w_5} + \frac{\lambda_a S_3 y_{a_6}}{\mathrm{d}x})}{m_a c_a} \tag{27}$$

$$\omega_{a_6} = \frac{(2u_{d_3} + \alpha_w S_6 y_{w_6} + \frac{\lambda_a S_3 y_{a_5}}{\mathrm{d}x})}{m_a c_a} \tag{28}$$

$$A_{a_{n1}} = \{(\alpha + 4\epsilon_a \sigma T_0^3)(S_1 + S_2 + S_3 - 2S_4 - S_5) + \alpha_w S_6 + \frac{\lambda_a S_3}{\mathrm{d}x}\}/m_a c_a \tag{29}$$

$$A_{a_{n2}} = \frac{\{6\epsilon_a \sigma T_0^2 (S_1 + S_2 + S_3 - 2S_4 - S_5)\}}{m_a c_a} \tag{30}$$

$$A_{a_{n3}} = \frac{\{4\epsilon_a \sigma T_0 (S_1 + S_2 + S_3 - 2S_4 - S_5)\}}{m_a c_a} \tag{31}$$

$$A_{a_{n4}} = \frac{\{\epsilon_a \sigma (S_1 + S_2 + S_3 - 2S_4 - S_5)\}}{m_a c_a}. \tag{32}$$

2.10 Modeling of tube inside the microreactor

Fig. 4 shows the model of tube inside a microreactor. The fundamental equation of tube is shown as

$$\frac{\partial T}{\partial t} = \alpha \frac{\partial^2 T}{\partial X^2}. \tag{33}$$

By using (33), thermal conduction equation of tube inside the microreactor is shown as Part $W_k (k = 1, 2, 3, 4, 5, 6)$.

$$\text{Part } W_1 : \frac{\mathrm{d}(T_0 - T_{w_1}) m_w c_w}{\mathrm{d}t} = \alpha_w S_6 (T_{w_1} - T_{a_1}) + \frac{2\lambda_w S_5 \{(T_{w_0} - T_{w_2}) - (T_{w_0} - T_{w_1})\}}{\mathrm{d}x^2} \tag{34}$$

$$\text{Part } W_2 : \frac{\mathrm{d}(T_0 - T_{w_2}) m_w c_w}{\mathrm{d}t} = \alpha_w S_6 (T_{w_2} - T_{a_2}) + \frac{2\lambda_w S_5 \{(T_{w_0} - T_{w_1}) + (T_{w_0} - T_{w_3}) - (T_{w_0} - T_{w_2})\}}{\mathrm{d}x^2} \tag{35}$$

$$\text{Part } W_3 : \frac{\mathrm{d}(T_0 - T_{w_3}) m_w c_w}{\mathrm{d}t} = \alpha_w S_6 (T_{w_3} - T_{a_3}) + \frac{2\lambda_w S_5 \{(T_{w_0} - T_{w_2}) + (T_{w_0} - T_{w_4}) - (T_{w_0} - T_{w_3})\}}{\mathrm{d}x^2} \tag{36}$$

$$\text{Part } W_4 : \frac{\mathrm{d}(T_0 - T_{w_4}) m_w c_w}{\mathrm{d}t} = \alpha_w S_6 (T_{w_4} - T_{a_4}) + \frac{2\lambda_w S_5 \{(T_{w_0} - T_{w_3}) + (T_{w_0} - T_{w_5}) - (T_{w_0} - T_{w_4})\}}{\mathrm{d}x^2} \tag{37}$$

$$\text{Part } W_5 : \frac{\mathrm{d}(T_0 - T_{w_5}) m_w c_w}{\mathrm{d}t} = \alpha_w S_6 (T_{w_5} - T_{a_5}) + \frac{2\lambda_w S_5 \{(T_{w_0} - T_{w_4}) + (T_{w_0} - T_{w_6}) - (T_{w_0} - T_{w_5})\}}{\mathrm{d}x^2} \tag{38}$$

$$\text{Part } W_6 : \frac{\mathrm{d}(T_0 - T_{w_6}) m_w c_w}{\mathrm{d}t} = \alpha_w S_6 (T_{w_6} - T_{a_6}) + \frac{2\lambda_w S_5 \{(T_{w_0} - T_{w_5}) - (T_{w_0} - T_{w_6})\}}{\mathrm{d}x^2}. \tag{39}$$

Define $y_{w_k} = T_0 - T_{w_k} (k = 1, 2, 3, 4, 5, 6)$ and are transformed as

$$\text{Part } W_k : \frac{\mathrm{d}y_{w_k}}{\mathrm{d}t} = \omega_{w_k} - A_{w_k} y_{w_k}. \tag{40}$$

Here, ω_{w_k} and $A_{w_k} (k = 1, 2, 3, 4, 5, 6)$ are shown as

$$\omega_{w_1} = \frac{\alpha_w S_6 y_{a_1} + \frac{2\lambda_w S_5 y_{w_2}}{\mathrm{d}x^2}}{m_w c_w} \tag{41}$$

$$\omega_{w_2} = \frac{\alpha_w S_6 y_{a_2} + \frac{2\lambda_w S_5 (y_{w_1} + y_{w_3})}{\mathrm{d}x^2}}{m_w c_w} \tag{42}$$

$$\omega_{w_3} = \frac{\alpha_w S_6 y_{a_3} + \frac{2\lambda_w S_5 (y_{w_2} + y_{w_4})}{\mathrm{d}x^2}}{m_w c_w} \tag{43}$$

$$\omega_{w_4} = \frac{\alpha_w S_6 y_{a_4} + \frac{2\lambda_w S_5 (y_{w_3} + y_{w_5})}{\mathrm{d}x^2}}{m_w c_w} \tag{44}$$

$$\omega_{w_5} = \frac{\alpha_w S_6 y_{a_5} + \frac{2\lambda_w S_5 (y_{w_4} + y_{w_6})}{\mathrm{d}x^2}}{m_w c_w} \tag{45}$$

$$\omega_{w_6} = \frac{\alpha_w S_6 y_{a_6} + \frac{2\lambda_w S_5 y_{w_5}}{\mathrm{d}x^2}}{m_w c_w} \tag{46}$$

$$A_{w_k} = \frac{\frac{2\lambda_w S_5}{\mathrm{d}x^2} + \alpha_w S_6}{m_w c_w}. \tag{47}$$

3 Control system design for the microreactor process

Fig. 5 shows the cooling control system of microreactor based on right coprime factorization. In this process, heat transfers from Part A_1 to Part W_1. The operator G_a means heat transfer from each part.

Part A_1 to Part A_6 of process are shown in (48). Similarly, Part W_1 to Part W_6 of process are shown in (49). Then, z_{a_n} and z_{w_k} mean input signal of P_{a_n} and P_{w_k}, y_{a_n} and y_{w_k} means the output of P_{a_n} (n=1–6) and P_{w_k} (k=1–6).

$$P_{a_n} : \dot{y}_{a_n} = \frac{z_{a_n}}{m_a c_a} + \sum_{m=1}^{4} (-1)^m A_{a_{nm}} y_{a_n}^m \tag{48}$$

$$P_{w_k} : \dot{y}_{w_k} = \frac{z_{w_k}}{m_w c_w} - A_{w_{k1}} y_{w_k}. \tag{49}$$

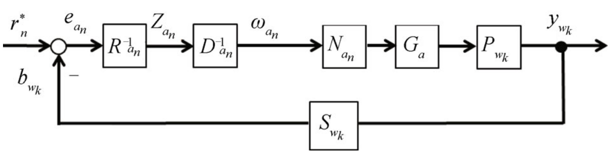

Fig. 5 Microreactor cooling system

4 Designed control system

P_{a_n} are divided into stable operator N_{a_n} and invertible stable operator $D_{a_n}^{-1}$ based on operator theory. N_{a_n} and

$D_{a_n}^{-1}$ are shown as

$$N_{a_n}:\ \begin{cases} \dot{x}_{a_n}(t) = \omega_{a_n}(t) + \sum_{m=1}^{4}(-1)^m A_{a_n m} y_{a_n}^m \\ y_{a_n}(t) = x_{a_n}(t) \end{cases} \tag{50}$$

$$D_{a_n}^{-1}:\ \omega_{a_n}(t) = \frac{z_{a_n}(t)}{m_a c_a}. \tag{51}$$

Fig. 6 shows the system of microreactor that satisfies the Bezout identity. The Bezout identity is shown as (52). S_{w_k}, R_{a_n} are designed controllers, where there are a stable operator and a stable invertible operator respectively, I means a unimodular operator.

$$S_{w_k}\tilde{N}_n + R_{a_n}D_{a_n} = I \tag{52}$$

$$\tilde{N}_n = N_{a_n}G_a P_{w_k}. \tag{53}$$

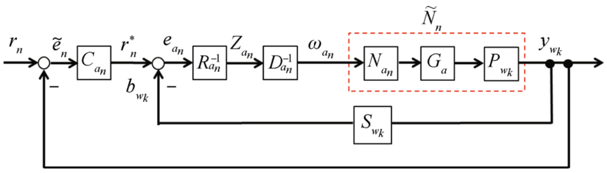

Fig. 6 System with tracking controller

When stable operator S_{w_k} and R_{a_n} are designed for satisfying the Bezout identity, $D_{a_n}^{-1}$ and $\tilde{N}_n$ are right coprime factorization. Here, the microreactor cooling control system is BIBO stable. S_{w_k} and R_{a_n} are designed as follows by using arbitrary constant B_n.

$$S_{w_k}: b_{w_k} = (1-B_n)(N_{a_n}^{-1}G_a^{-1}P_{w_k}^{-1}) \tag{54}$$

$$R_{a_n}^{-1}: z_{a_n} = \frac{m_a c_a}{4B_n}e_{a_n}. \tag{55}$$

4.1 Improvement of tracking performance in microreactor systems

Tracking controller C_{a_n} is used for achieving tracking performance of the system. Here, C_{a_n} is designed as

$$C_{a_n}(\tilde{e}_n)(t) = k_{pa_n}\tilde{e}_n(t) + k_{ia_n}\int_0^t \tilde{e}_n(\tau)\mathrm{d}\tau. \tag{56}$$

5 Simulation results

This section gives simulation results to confirm the effectiveness of the designed systems. The parameters of simulation are shown in Table 2. Simulation results are shown in Figs. 7 – 9. The color versions of Figs. 7–9 for simulation and Figs. 10–12 for experiment in this paper are available online.

The purpose of this simulation is to control the tube temperature to the target temperature. Target temperature is 24 for boxs 1 – 3.

5.1 Discussion

In Figs. 7 to 9, the temperature of tube is tracking the target value of 24°C. Also, temperature of aluminum is shown in the above figures. Temperature difference means the temperature between tube and aluminum. Temperature of aluminum is about 2°C lower than the temperature of tube. Temperature of tube moves in the same way as temperature of aluminum moves. From this, it can be said that the temperature of tube is affected by the temperature of aluminum.

Table 2 Parameters of simulation

Parameters	Values
Target temperature	297 K (24°C)
Outside temperature	T_0 = 300 K (27°C)
Initial water temperature	T_{w0} = 323 K (50°C)
Designed parameters	$B_1 = B_2 = B_3 = 0.6$
Gain of P_1	$K_{P_1} = 5.0$
Gain of I_1	$K_{I_1} = 0.005$
Gain of P_2	$K_{P_2} = 6.0$
Gain of I_2	$K_{I_2} = 0.003$
Gain of P_3	$K_{P_3} = 7.0$
Gain of I_3	$K_{I_3} = 0.001$
Simulation time	600 s
Sampling time	0.1 s

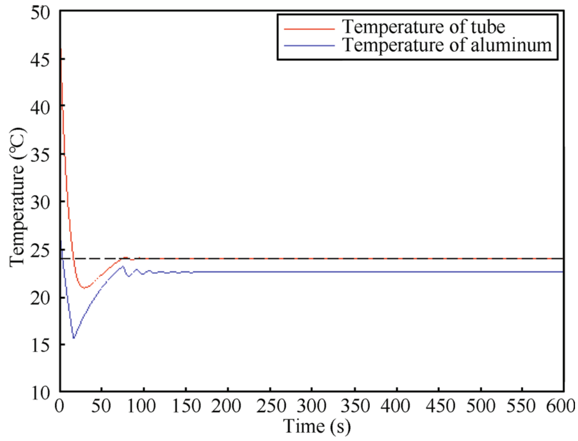

Fig. 7 Temperature of tube in box 1

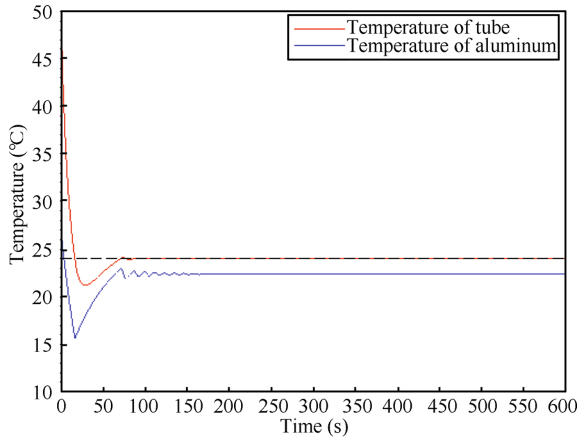

Fig. 8 Temperature of tube in box 2

6 Experimental results

This section gives the experimental results to confirm the effectiveness of the proposed system. The purpose of this experiment is to control the water temperature inside the tube to target value. The microreactor group experimental setup is made of three aluminum boxes. Peltier devices are set to each aluminum box to control the water temperature of tube inside the aluminum box. In this experiment, water is not flowing. Table 3 shows the parameters of this experiment. Experimental results are shown in Figs. 10–12. Target temperature is 12°C which starts from 15°C for boxs 1–3. Figs. 10–12 shows the water temperature inside the tube. Broken line in Figs. 10–12 shows the target temperature of the tube. From the experiment results, tube in aluminum boxes is tracking the target temperature difference. The effectiveness of proposed system is shown.

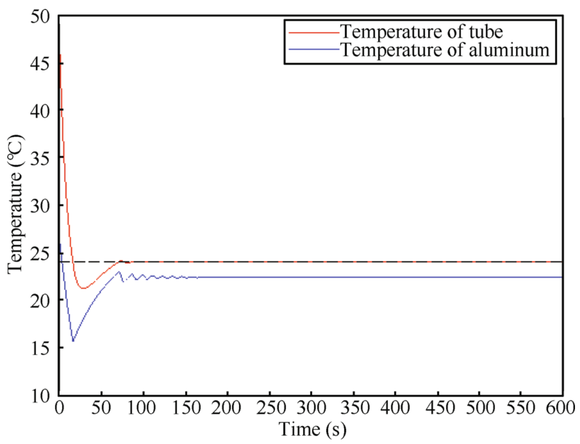

Fig. 9 Temperature of tube in box 3

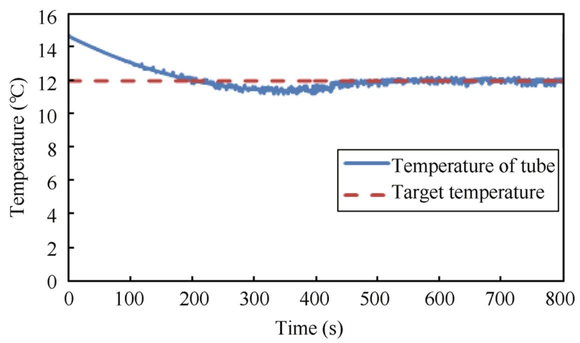

Fig. 10 Experimental result on temperature of of tube in box 1

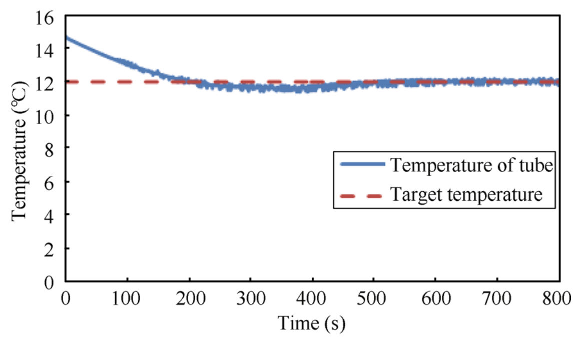

Fig. 11 Experimental result on temperature of tube in box 2

7 Conclusions

In this paper, the microreactor group actuated by Peltier devices is proposed. The main purpose is to control the temperature of the tube inside the microreactor group. First, the aluminum box and tube that constitute the microreactor group is modeled by considering conduction, convection, and radiation. Second, the operator based nonlinear feedback cooling control system is designed. Finally, the effectiveness of the proposed model and designed system is confirmed by experimental results.

Table 3 Parameters of experiment

Parameters	Values
Temperature difference	276 K (3°C)
Outside temperature	298 K (25°C)
Initial water temperature	288 K (15°C)
Experiment time	800 s
Sampling time	0.3 s
Designed parameters	$B_1 = 0.60$
Designed parameters	$B_2 = 0.65$
Designed parameters	$B_3 = 0.63$
Gain of P_1	$K_{P_1} = 39.0$
Gain of I_1	$K_{I_1} = 0.0005$
Gain of P_2	$K_{P_2} = 34.0$
Gain of I_2	$K_{I_2} = 0.0003$
Gain of P_3	$K_{P_3} = 30.0$
Gain of I_3	$K_{I_3} = 0.0001$

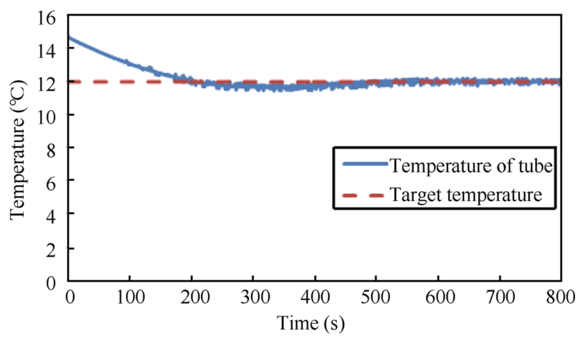

Fig . 12 Experimental result on temperature of tube in box 3

References

[1] D. M. Rowe. *Thermoelectrics Handbook: Macro to Nano*, Boca Raton, USA: CRC Press, 2005.

[2] W. Ehrfeld, V. Hessel, H. Lowe. *Microreactors: New Technology for Modern Chemistry*, New York, USA: Wiley-VCH, 2000.

[3] N. Kadowaki, K. Suzumori, A. Muto. Three-port valve to generate length-controllable slug flow for chemical process. *Transactions of the Japan Society of Mechanical Engineers, Series C*, vol. 76, no. 763, pp. 734–740, 2010. (in Japanese)

[4] W. Seifert, M. Ueltzen, C. Strumpel, W. Heiliger, E. Muller. One-Dimensional modeling of a Peltier element. In *Proceedings of International Conference on Thermoelectrics*, IEEE, Beijing, China, pp. 439–443, 2001.

[5] M. C. Deng, A. Inoue, K. Ishikawa. Operator-based nonlinear feedback control design using robust right coprime factorization. *IEEE Transactions on Automatic Control*, vol. 51, no. 4, pp. 645–648, 2006.

[6] M. C. Deng. *Operator-Based Nonlinear Control Systems: Design and Applications*, New York, USA: Wiley-IEEE Press, 2014.

[7] M. C. Deng, S. Wen, A. Inoue. Operator-based robust nonlinear control for a Peltier actuated process. *Measurement and Control*, vol. 44, no. 4, pp. 116–120, 2011.

[8] M. C. Deng, S. H. Bi. Operator-based robust nonlinear control system design for MIMO nonlinear plants with unknown coupling effects. *International Journal of Control*, vol. 83, no. 9, pp. 1939–1946, 2010.

[9] K. Umemoto, M. C. Deng. Operator-based non-linear control system design for unstable plants with input saturation. *International Journal of Advanced Mechatronic Systems*, vol. 3, no. 4, pp. 297–303, 2011.

[10] S. H. Bi, M. C. Deng. Operator-based robust control of MIMO aluminium plate thermal process. *International Journal of Computer Applications in Technology*, vol. 44, no. 4, pp. 249–256, 2012.

[11] C. A. Jiang, M. C. Deng, A. Inoue. Robust stability of nonlinear plants with a non-symmetric Prandtl-Ishlinskii hysteresis model. *International Journal of Automation and Computing*, vol. 7, no. 2, pp. 213–218, 2010.

[12] M. C. Deng, S. Wen, A. Inoue. Operator-based robust nonlinear control for a Peltier actuated process. *Measurement and Control*, vol. 44, no. 4, pp. 116–120, 2011.

[13] S. J. Wen, M. C. Deng, S. H. Bi, D. Y. Wang. Operator-based robust nonlinear control and its realization for a multi-tank process by using a distributed control system. *Transactions of the Institute of Measurement and Control*, vol. 34, no. 7, pp. 891–902, 2012.

[14] S. Kawahata, K. Takahashi, M. C. Deng. Nonlinear water temperature control of three connected microreactors actuated by Peltier devices. In *Proceedings of the 11th International Conference on Networking, Sensing and Control*, IEEE, Miami, USA, pp. 542–547, 2014.

[15] K. Takahashi, S. J. Wen, M. Sanada, M. C. Deng. Nonlinear cooling control for a Peltier actuated aluminum plate thermal system by considering radiation heat transfer. In *Proceedings of International Conference on Advanced Mechatronic Systems*, IEEE, Tokyo, Japan, pp. 18–23, 2012.

[16] S. Kawahata, M. C. Deng, K. Takahashi. Nonlinear water temperature control experiment for microreactor group actuated by Peltier devices. In *Proceedings of the International Conference on Advanced Mechatronic Systems*, IEEE, Kumamoto, Japan, pp. 7–10, 2014.

Shotaro Kawahata received the B. Sc. degree in applied electrical and electronic engineering from Tokyo University of Agriculture and Technology, Japan in 2014. He is currently a master student in the Graduate School of Engineering of Tokyo University of Agriculture and Technology, Japan.

His research is nonlinear control system design.

E-mail: 50014645111@st.tuat.ac.jp

ORCID iD: 0000-0002-6174-6055

Ming-Cong Deng received the Ph. D. degree in systems science from Kumamoto University, Japan in 1997. From 1997 to 2000, he was with Kumamoto University as an assistant professor. From 2000 to 2001, he was in University of Exeter, UK, and then spent one year at the Communication Science Laboratories, Nippon Telegraph and Telephone Corporation (NTT). Since the end of 2002 to September of 2010, he worked at Okayama University, where he was an assistant professor and then an associate professor. He is currently a professor of Tokyo University of Agriculture and Technology, Japan.

His research interests include operator-based nonlinear system modeling, control and fault detection, strong stability-based control, and robust parallel compensation.

E-mail: deng@cc.tuat.ac.jp (Corresponding author)

ORCID iD: 0000-0001-7411-6602